Jurnal Engine: Energi, Manufaktur, dan Material e-ISSN: 2579-7433
Anugrah, Wisnujati & Anggara, Vol.7, No.2, November 2023: Hal. 01- 06

Delta EC Simulation on Influence of Resonator Length in Close-Open Standing Wave Thermoacoustic Engine

[1)]*Rinasa Agistya Anugrah, [2)]Andika Wisnujati, [3)]Fajar Anggara

[(1,2)]Department of Automotive Engineering Technology, Universitas Muhammadiyah Yogyakarta, Jl. Brawijaya, Tamantirto, Kasihan, Bantul, D.I. Yogyakarta 55183 Indonesia
[(3)]Department of Mechanical Engineering, Faculty of Engineering, Universitas Mercu Buana, Jl. Meruya Selatan No. 1 Kembangan, Jakarta, 11650 Indonesia
**Email: rinasaanugrah@umy.ac.id*

Diterima: 20.04.2023, Disetujui: 11.10.2023, Diterbitkan: 22.10.2023

ABSTRACT

Many applications of thermoacoustic engine in engineering. With the pressure of it, the energy can be harvested and can be converted to many other needs of energies like electrical energy. Energy in thermal form is converted to become acoustic energy and subsequently used to activate bidirectional turbine. Resonator is very influential toward the power of thermoacoustic engine. Simulation study with Delta EC fit to make predictions acoustic power as representative performance in thermoacoustic engine with close-open type and standing wave of oscillation. In this study, the material of the resonator is made from stainless-steel duct with diameters size of 50.8 mm with three variations of the length. The Standing-Wave Thermoacoustic Engine (SWTE) generates acoustic energy from temperature gradient of 315 – 993 K. In this simulation Acoustic Power decreased when resonator length was extended. The shortest resonator had acoustic power 50.4 W, and the longest resonator had acoustic power 35.7 W.

Keywords: SWTE, Simulation, Delta EC, Acoustic Power, Resonator Length.

ABSTRAK

Banyak aplikasi mesin termoakustik di bidang teknik. Dengan tekanan sebesar itu, energi dapat dipanen dan dapat diubah menjadi berbagai kebutuhan energi lainnya seperti energi listrik. Energi dalam bentuk panas diubah menjadi energi akustik dan selanjutnya digunakan untuk mengaktifkan turbin dua arah. Resonator sangat berpengaruh terhadap daya mesin termoakustik. Studi simulasi dengan Delta EC cocok untuk membuat prediksi kekuatan akustik sebagai kinerja perwakilan pada mesin termoakustik dengan tipe buka-tutup dan gelombang osilasi berdiri. Pada penelitian ini material resonator dibuat dari pipa stainless steel dengan ukuran diameter 50,8 mm dengan tiga variasi panjang. Standing-Wave Thermoacoustic Engine (SWTE) menghasilkan energi akustik dari gradien temperatur 315 – 993 K. Pada simulasi ini Acoustic Power menurun ketika panjang resonator diperpanjang. Resonator terpendek memiliki daya akustik 50,4 W, dan resonator terpanjang memiliki daya akustik 35,7 W.

Kata Kunci: SWTE, Simulasi, Delta EC, Daya Akustik, Panjang Resonator.

I. Introduction

Thermoacoustic devices have come a long way in recent decades, ending the relentless lure of similar systems in the industry. Thermoacoustic heat engines (TAHEs) will soon replace the last compressor-driven motors used as drivers in cryocoolers. The increasing importance in the thermoacoustic field is the result of using no unusual matters, motionless parts, compatible efficiencies and utilize of environmental-friendly media. Similarly, TAHE should be incorporated into bi-directional turbine and generator units to produce electrical energy.

A thermoacoustic engine has contents motionless parts, but the acoustic excitation of heat flow and the production of acoustic perform represent the temporal stages of a thermodynamic process. In consequence of the turn-out of the machinal means, fluid and stack lisps. The fluid pack in the thermoacoustic engine replaces transference and healer as the pressure changes. To yield a thermoacoustic clout, these vibrations must come to pass near solid surfaces and heat must be shifted to and out of the superficies. As ballot waves pass by way of a gasiform means in narrow ducts, temperature is removed through the gas towards the walls, creating emphasis and healer fluctuations. Conversely, changes in emphasis and healer render ballot waves. The merger of entire these processes creates a rich 'thermoacoustic' effect. This is shown in Figure 1.

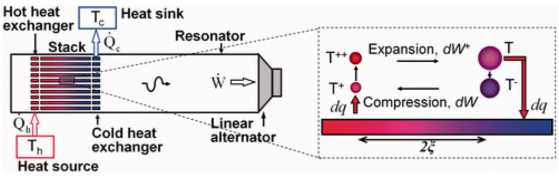

Figure 1. A Phenomenon of Thermoacoustic Effects (Jaworski & Mao, 2013)

The effects of operational parameters, parameter of geometric, and working fluids on TAHE accomplishment have been extensively described in many research studies. These investigations varied the stack position, stack length, lisp gap, lisp thickness, heating power, tilt angle of the TAHE, and resonator geometry such as tapers and loops to vary the length of the TAHE. evaluated the performance of Also, the basic harmonic component, onset and decay features of thermoacoustic oscillations are well represented. To operate thermoacoustic refrigerators, TAHE have to generate peak resonant frequencies with increased pressure amplitude, what is well-thought-of a key criterion for measuring the intension of vibration. True a system is able to be realized by the development of this thermoacoustic engine.

Researchers (Bai et al., 1998) studied the performance of a thermoacoustic engine by varying the working medium, pressure, cavity length and heater temperature sans in view of the influences of variable loads to the system. Two researchers (Zhou & Matsubara, 1998) conducted experimentations with a fixed heat input and inspected the distiction of the onset and decay temperatures. Various resonator geometries as well as loop tubes (Yu et al., 2003) and tapered resonators (Tang et al., 2006) have also been used to study the accomplishment of thermoacoustic engines. Then also the next researchers (Jintao et al., 2007) used porous ceramic honeycomb stacks to study the effect of frequency and amplitude regarding stack position on the roundly achievement of a thermoacoustic engine. Research (Masood et al., 2007) explored the achievement of thermoacoustic refrigerators by the effects of gas drawback by little and major thermal contact regions midst the chimney and heat exchanger and sans a heat exchanger. They said that a heat exchanger by a larger thermal contact region goes up the heat exchange midst the heat exchange fluid and the stack but drops the cooling capacity and increases the workload of the stack caused by intensify gas drawback. I found that it lets.

A study (Mehta et al., 2011) found that geometric (length of stack, position of stack and cavity length) and driving parameters (filling pressure, heat input, hot-end temperature) affect standing-wave thermoacoustic. Reported impact on motor performance. Afterward there is a study (Qiu et al., 2012) which conducted research and proposed a numeral designl based on thermodynamic elucidation to predict the onset temperature by contrasting the lisp gap, boost pressure and cavity length. The developed design fitted the experimental conditions well. Thermoacoustic engine performance is influenced by five key variables: position of stack, length of stack, length of resonator, lisp gap, and lisp thickness. Then previous research also (Hariharan et al., 2012) established an experiment with thermoacoustic engine performance variables, called position of stack and length of stack. The effect of PT and PS on thermoacoustic engine achievement was not reported in the previously cited article. Hence, the primary aim of this work is to obtain the effect of PT with diverse PS and cavity length. Thin plate stacks consume more thermal energy than thick plates to generate vibrations and affect experimental results such as cavity length. Previous research (Mehta et al., 2011) reported that geometric (length of stack, position of stack and cavity length) and driving parameters (input of heat, charging pressure and temperature on hot end) affect the accomplishment of standing wave thermoacoustic engines in terms of acoustic power and pressure ratio. Reported impact. A previous study (Hao et al., 2011), held theoretical and experimental study of the achievement of a standing-wave thermoacoustic engine by varying the working fluid at dissimilar pressures and dissimilar combinations. By changing the plate gap, boost pressure and cavity length. The effect of staple wire mesh porosity on TAHE performance was not reported in the previously cited publications. Also, the change in cavity length can be used for purposes other than the above.

II. Method of Simulation

Delta EC ("Design Environment for Low Amplitude Thermoacoustic Energy Conversion"), invented by Ward and Swift, is usually applied to optimize thermoacoustic devices numerically and appraise their efficiency. This code breaks the one-dimensional gas wave equation based on a low-amplitude acoustic estimation of arranging geometry. Delta EC is able to obtain frequency resolutions from the sound pressure amplitude, the onset temperature difference, and the open geometry of the thermoacoustic engine. In the provide analysis, the laminated sheet thickness, lamellar spacing and resonator length were varied and the appropriate output were obtained from the simulations. We make comparison between the simulation of the Delta EC results with the experimental results.

TAHE simulation studies were performed using the low amplitude thermoacoustic energy conversion computer program evolved by Greg Swift and his colleagues, or more generally the design environment of Delta EC. For appraising the efficiency of thermoacoustic equipment, this Delta EC is a capable instrument for modeling and designing thermoacoustic and other one-dimensional acoustic equipment. This program resolves the one-dimensional Rott wave equation (Rott, 1980) for a given gas pressure and volume velocity, solves the Rott enthalpy equation, and computes the air motion in the thermoacoustic stack based on a low acoustic amplitude custom geometry estimation. To do. Calculate the temperature profile of . The main sections took to construct a double TAHE with delta EC are "BEGIN, DUCT, HX, STKSLAB, SOFTENED, and HARDENED". Among various stack geometries such as "STKCIRC, STKRECT, STKSLAB, STKSCREEN and STKPIN, STKSLAB" was chosen for the simulation. This is to reflect collateral plate geometry. Since the current system is a closed half-wave twin TAHE (symmetric system), SOFTENED and HARDENED segments were used for the simulation. Here the complex pressure amplitude should be zero in the SOFTEND segment, and the problematic volumetric flow rate should be zero. HARDENED - segment.

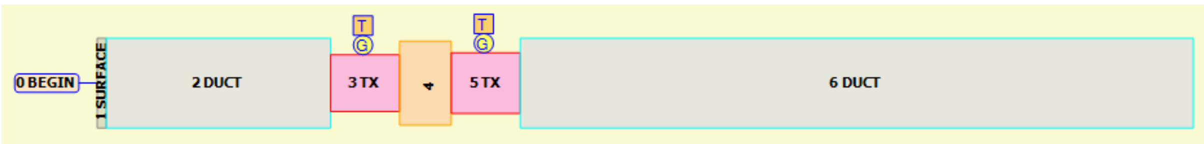

Figure 2. DeltaEC Thermoacoustic Heat Engine Simulation Model

Since the resonator diameter was 0.0525 m in this study, the area willing to air and the swirl of the resonator were calculated and placed in the DUCT segment. The cross-sectional area, perimeter, cross-sectional ratio, length, half-plate gap, and half-plate thickness of the stack and heat exchanger are inserted into the Delta-EC according to the experimental geometry. The clogging rate was 0.5 when calculated with a plate thickness of 0.0005m and a plate gap of 0.0005m. The chimney and heat exchanger lengths were changed to 0.03m and 0.04m for STKSLAB and HX segments, serially. Stainless steel and copper materials were chosen from the STKSLAB and HX Delta EC software databases, respectively. Simulations were performed by varying the length of the resonator. 0.39 m, 0.79 m, and 1.17 m, and the experiment used frequency, temperature, and pressure amplitude as estimates for the BEGIN statement that the system's output was set. Symmetric systems were connected via SOFTEND segments. Set the real and imaginary parts of the intrinsic impedance of the HARDENED segment as targets for the system. In the current simulation, the working fluid is only normal air to keep track of the achievement of standing wave TAHE. The modelling of TAHE is shown in Figure 2.

Delta EC is involved to one-dimensional orders of either acoustic or thermoacoustic matters, named by segment, thus Delta EC's "wave" equation also in level one-dimensional. It is able to regard a time dependence of Re[$e^{i\omega t}$], ergo the "wave" equation is able to be taken as the second order Hemholtz differential equation toward the complex pressure amplitude $p_1(x)$. In its most great form, in an x-independent cross-sectional area A, sans viscous or thermal-hysteresis losses, as follows (Clark et al., 2007):

$$p_1 + \frac{a^2 d^2 p_1}{\omega^2 dx^2} = 0 \qquad (1)$$

It is frequently prone to reflect of this second-order equation as two in pairs first-order equations in pressure p_1 & volume flow rate U_1:

$$\frac{dp_1}{d_x} = -\frac{i\omega\rho_m}{A} U_1 \qquad (2)$$

$$\frac{dU_1}{dx} = -\frac{i\omega A}{\rho_m a^2} p_1 \qquad (3)$$

The dp_1/dx equation is derived from momentum equation and the dU_1/dx equation is derived from the continuity equation of fluid mechanics. In this form, the equations are ripe to simultaneous numerical integration along the axial position coordinate x to deliver solutions $p_1(x)$ and $U_1(x)$. And the result of acoustic power Edot ($\dot{E}$) is calculated by:

$$\dot{E} = \frac{1}{2} Re[p_1 \tilde{U}_1] \qquad (4)$$

III. Research Result

In results of this simulation served datas the distribution of acoustic power throughout length of resonator as provided in Figure 3-5. Figure 3 shows the acoustic power relationship produced by a one-cavity thermoacoustic engine. Figure 4 shows the relationship between the acoustic power produced by two-cavity and three-cavity thermoacoustic engines. The distribution of the three resonators shows the same, the one that comes last reduces the sound power. The point at the edge of each resonator had the lowest acoustic power for each resonator of the three resonators.

Based on previous research (Hariharan et al., 2013), they explain their research, if the resonator length has been extended, the frequency woud be decreased. Decreasing in frequency was along signified with reducing acoustic power. Therefore in the end of resonator in this simulation presented lowest acoustic power.

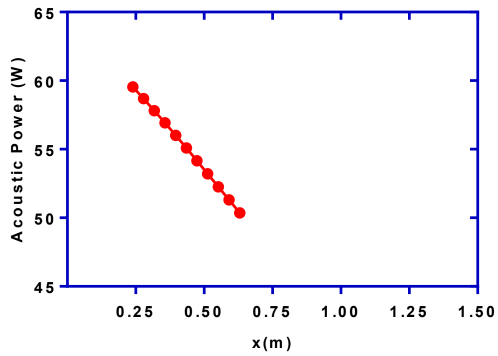

Figure 3. Simulation of 1 resonator, distribution acoustic power throughout length of resonator

According to previous research, which was conducted by experimental method, the result has the same trend as this simulation method. The longer the resonator length the smaller the value of acoustic intensity (Anugrah et al., 2018). So, the acoustic intensity is reflected how much the acoustic power is because it is represented by the power divided by cross-sectional area. However, the trend of resonator length is also the same both experiment and simulation. Based on Figure 2, we can see that the highest power is at 0.25 m with the value is 60 W. It is the same for all variations, the highest power is always at 0.25 m of resonator length.

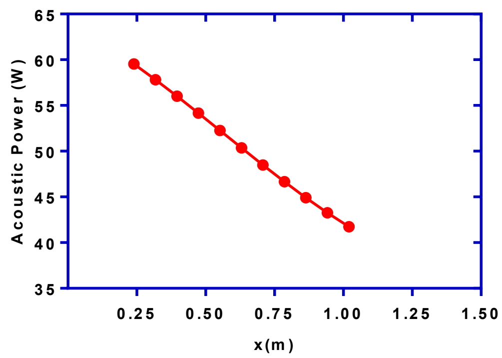

Figure 4. Simulation of 2 resonators, distribution acoustic power throughout length of the resonator

Figure 5 shows the trend on third variant that is longer than aboves. The acoustic powers which are at up to 1.25 m are lower than 40 W. So, it has been proved that the longer the resonator length, the lower of acoustic power. It happened because of the frequency, the one of the functions of acoustic power parameter which is caused also by the extension of resonator length. The frequency depends on resonator length which the more increased of resonator length the more decreased of frequency.

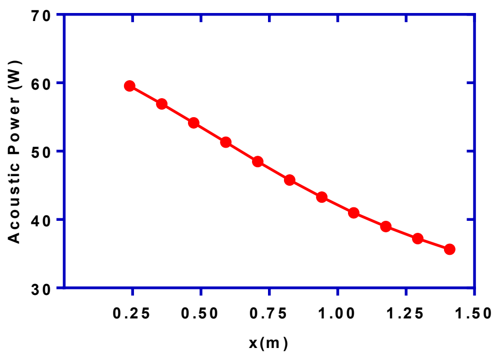

Figure 5. Simulation of 3 resonators, distribution acoustic power throughout length of the resonator

In Figure 6, Acoustic power decreased when resonator length was extended. The shortest resonator had acoustic power 50.4 W, and the longest resonator had acoustic power 35.7 W. The study which was conducted by a researcher (Hariharan et al., 2012) has also explained in their paper that acoustic power would decrease when resonator length would have been extended. It happened because when the resonator was extended so the frequency, and the function of acoustic power (Edot / $\dot{E}$), was decreased too.

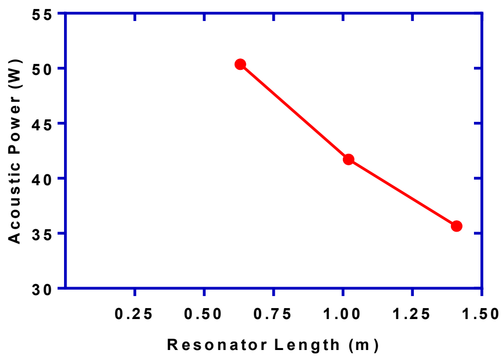

Figure 6. The effect of variations of resonator length on acoustic power

IV. Concluding Remark

In this simulation Acoustic Power decreased when resonator length was extended. The shortest resonator had acoustic power 50.4 W, and the longest resonator had acoustic power 35.7 W. It can be concluded that the results obtained from the simulations were consistent with the theoretical results of the experimental studies.

References

Anugrah R. A., Widyaparaga A., Miasa I. M., Waluyo J., Sugiyanto, and Kamal S., "Experimental study on performance of standing-wave thermoacoustic engine at different tilted angles and resonator length," *AIP Conf. Proc.*, vol. 2001, no. August, 2018, doi: 10.1063/1.5050013.

Atchley A.A., Bass H.E., Hofler T.J., Lin H.T. Study of a thermoacoustic prime mover below onset of self-oscillation. J Acoust Soc Am 1992;91:734–43.

Bai X., Jin T., Chen G.B. Experimental study on thermoacoustic primemover. In: Proceedings of the conference on cryogenics and refrigeration. Hangzhou, China; 1998. p. 522–5.

Clark, J.P., Ward, W. C., Swift, G. W. (2007). Design environment for low-amplitude thermoacoustic energy conversion (DeltaEC). The Journal of the Acoustical Society of America, 122(5), 3014. https://doi.org/10.1121/1.2942768

Hao X.H., Ju Y.L., Behera U., Kasthurirengan S. Influence of working fluid on the performance of standing wave thermoacoustic primemover. Cryogenics 2011;51:559–61.

Hariharan N.M., Sivashanmugam P., Kasthurirengan S. Experimental and theoretical investigation of thermoacoustic prime mover. HVAC&R Res, in press. 2012

Hariharan N.M., Sivashanmugam P., Kasthurirengan S. Influence of stack geometry and resonator length on the performance of thermoacoustic engine. Applied Acoustics 2012;73:1052-1058.

Hariharan NM, Sivashanmugam P., Kasthurirengan S. Influence of stack geometry and resonator length on the performance of thermoacoustic engine. Computer & Fluids 2013;75:51-55.

Jaworski, A.J. & Mao, X. 2013. *Development of Thermoacoustic Devices for Power Generation and Refrigeration.* Proc. IMechE Part A: J. Power and Energy, Vol. 227 No. 7, hal. 762-782

Masoud A.M.H, Kamran S., Bhat R.B. The impact of gas blockage on the performance of a thermoacoustic refrigerator. Exp Therm Fluid Sci 2007;32:231–9.

Mehta S.M., Desai K.P., Naik H.B., Atrey M.D. Design of standing wave type thermoacoustic prime mover for 300 Hz operating frequency. In: International cryocooler conference, Inc., Boulder, CO; 2011. p. 343–52.

Qiu L.M., Lai B.H., Li Y.F., Sun D.M. Numerical simulation of the onset characteristics in a standing wave thermoacoustic engine based on thermodynamic analysis. Int J Heat Mass Trans 2012;55:2200–3.

Rott N. Thermoacoustics. Adv Appl Mech 1980;20:135–74.

Tang K., Chen G.B., Jin T., Bao R., Li X.M. Performance comparison of thermoacoustic engines with constant-diameter resonant tube and tapered resonant tube. Cryogenics 2006;46:699–704.

Tao J., Bao-Sen Z., Ke T., Rui B., Guo-Bang C.. Experimental observation on a small-scale thermoacoustic prime mover. J Zhejiang Univ Sci A 2007;8:205–9.

Yu Z.B., Li Q., Chen X., Guo F.Z., Xie X.J., Wu J.H. Investigation on the oscillation modes in a thermoacoustic Stirling prime mover: mode stability and mode transition. Cryogenics 2003;43:687–91.

Zhou, S. & Matsubara, Y. Experimental research of thermoacoustic prime mover. Cryogenics 1998;387:813–22.